Second Order Extension of Power Amplifiers Behavioral Models for Accuracy Improvements

Georges Zakka El Nashef[#], François Torrès[#], Sébastien Mons[#], Tibault Reveyrand[#], Thierry Monédière[#], Edouard N'Goya[#], Raymond Quéré[#]

[#]*XLIM – C2S2/OSA departments UMR CNRS n06172, university of Limoges, 87060 Limoges, France*

Email: georges.zakka-el-nashef@xlim.fr

***Abstract*— In the design process of reconfigurable radars, it is required to study the interaction between antennas and the power amplifiers in order to quantify the distortion and predict the performances of power amplifier (PA) on TX-chains. This paper presents an accurate behavioral model for PAs, based on nonlinear scattering functions, which allows taking into account large output loading impedance mismatches, i.e. Voltage Standing Wave Ratio (VSWR) up to four. First application presented is a black box modeling technique limited to Taylor first order expansion dedicated to moderate VSWR (VSWR ≤ 3). Unfortunately, the first order model is not efficient enough, so a second application is presented, showing an accurate model expanded to Taylor second order in the case of large VSWR (VSWR > 3) which allows predicting circuit performances at system level and establishes a mixed simulation tool for a bilateral communication between amplifiers and antennas.**

I. INTRODUCTION

The active reconfigurable antennas devices require taking into account simultaneously both the circuit and the electromagnetic aspects. Thus, accurate modeling and simulation process are needed in order to take into account the interaction between PAs and antennas correctly. This paper focuses on establishing an accurate behavioral model for PAs, enabling to predict and analyze the impact of microwave components on system performances, especially on the problem of mismatching between antennas and PAs. This mismatching clearly affects the PAs performances in terms of gain (AM/AM) and phase (AM/PM), thus modifying the necessary weights applied to the array and degrading its efficiency and radiation performance. Therefore, a new technique is needed to take into account both effects (antennas and PAs).

Concerning the electromagnetic issues (Antennas), a technique was developed to determine the mismatching impedances (≠50Ω) of each element of the array according to the frequency and the pointing angle [1]. This technique takes into account the mutual coupling between array elements (antennas) and calculates the necessary weights in order to obtain an optimum radiation pattern (high gain and low side lobes levels). As stated above, this electromagnetic technique permits also to study the impact of the calculated mismatching impedances on the performances of the PA, these calculated impedances being used as load impedances for the PA. This study will give us clues on the behavior of the PA in presence of an antenna (characterized by the load impedance). Further explanation concerning this electromagnetic approach can be found in [4].

In this paper, we present two bilateral behavioral models of the PA, based on the Poly-Harmonic Distortion (PHD) model presented in [2]. First step is a model limited to the first order of Taylor expansion. Second one is an expanded Taylor development to the second order, leading to an accurate and efficient model in the case of large load impedances mismatches (i.e. VSWR > 3). In [2], a "black box" frequency-domain behavioral model, requiring no prior knowledge of the device physics or circuit configuration of the nonlinear component, was identified from real measurements on a wide-band microwave integrated circuits amplifier using a Vector Nonlinear Network Analyzer (VNNA). The measurements were experimentally demonstrated to be valid for small and large amplitude drive signals, correctly predict even and odd harmonics, and simulate accurately even into impedances different from the 50Ω environment in which the data were measured. However, our study aims at taking into account large output loading mismatches (VSWR >3) due to the design constraints of the antennas array, in which the radiating elements have a small inter-spacing between two consecutive component, therefore resulting in a high mutual coupling leading to a calculated impedances far away from 50Ω (i.e. large VSWR obtained). Both models presented in this paper are based on the PHD formulation, but the main difference is that our model concerns the load mismatches effects operating at fundamental frequency (8.2 GHz), without taking into account the harmonics generated by the nonlinear device. Therefore, the model identification algorithm is different as well.

Finally, the active circuit model limited to first order is implemented in Agilent Advanced Design System (ADS), where it will be validated on the antenna's operating frequency for different loading impedances up to VSWR=3. Then the second order model is validated by comparison with measurement results obtained on several loading impedance mismatches up to VSWR=4 and on some calculated impedances characterizing the radiating array as well.

II. NON LINEAR SCATTERING FUNCTIONS

A. Theory

The basics of nonlinear Scattering functions were introduced by J. Verspecht [3], and consist in defining a nonlinear relation for the [S] parameters:

$$\tilde{b}_i = [S_{ij}]_{Non-Linear} \cdot \tilde{a}_i \qquad (1)$$

where $\tilde{a}_i$ & $\tilde{b}_i$ are respectively the incident and reflected power waves and [S_{ij}] are the nonlinear scattering functions. Initially, in order to establish a bilateral nonlinear model, the memory effects are neglected, which means that this model is limited to the working frequency. This leads to write:

$$\tilde{b}_i = f_{NL}\{\Re e(\tilde{a}_1), \Im m(\tilde{a}_1), \Re e(\tilde{a}_2), \Im m(\tilde{a}_2)\} \qquad (2)$$

In order to simplify the model, we decided to make the assumption that the PA works in weakly non-linear condition ($a_2 << a_1$), and as a first step, to limit the Taylor expansion to the first order. The development of Taylor series limited to the first order enables us to write Equation (2) as follows:

$$\begin{aligned}\tilde{b}_i = f_{NL}(\vec{X}_0) &+ \left.\frac{\partial f_{NL}(\vec{X})}{\partial \tilde{a}_1}\right|_{\vec{X}=\vec{X}_0} \cdot \left(\tilde{a}_1 - \tilde{a}_1|_0\right) + \left.\frac{\partial f_{NL}(\vec{X})}{\partial \tilde{a}_1^*}\right|_{\vec{X}=\vec{X}_0} \cdot \left(\tilde{a}_1^* - \tilde{a}_1^*|_0\right) \\ &+ \left.\frac{\partial f_{NL}(\vec{X})}{\partial \tilde{a}_2}\right|_{\vec{X}=\vec{X}_0} \cdot \left(\tilde{a}_2 - \tilde{a}_2|_0\right) + \left.\frac{\partial f_{NL}(\vec{X})}{\partial \tilde{a}_2^*}\right|_{\vec{X}=\vec{X}_0} \cdot \left(\tilde{a}_2^* - \tilde{a}_2^*|_0\right)\end{aligned} \qquad (3)$$

where $\tilde{b}_i = f_{NL}\left(\tilde{a}_1, \tilde{a}_1^*, \tilde{a}_2, \tilde{a}_2^*\right)$, $\vec{X} = \left(\tilde{a}_1, \tilde{a}_1^*, \tilde{a}_2, \tilde{a}_2^*\right)$ and $\vec{X}_0 = \left(\tilde{a}_1|_0, \tilde{a}_1^*|_0, \tilde{a}_2|_0, \tilde{a}_2^*|_0\right)$. $\tilde{a}_2 \approx 0$, so $\tilde{a}_2^* \approx 0$.

The PA behavior thus depends only on incident wave $\tilde{a}_1$, and it is possible to write: $\vec{X} = \left(\tilde{a}_1, \tilde{a}_1^*, 0, 0\right)$. Equation (3) becomes:

$$\begin{aligned}\tilde{b}_i = f_{NL}(\vec{X}_0) &+ \left.\frac{\partial f_{NL}(\vec{X})}{\partial \tilde{a}_1}\right|_{\vec{X}=\vec{X}_0} \cdot \left(\tilde{a}_1 - \tilde{a}_1|_0\right) + \left.\frac{\partial f_{NL}(\vec{X})}{\partial \tilde{a}_1^*}\right|_{\vec{X}=\vec{X}_0} \cdot \left(\tilde{a}_1^* - \tilde{a}_1^*|_0\right) \\ &+ \left.\frac{\partial f_{NL}(\vec{X})}{\partial \tilde{a}_2}\right|_{\vec{X}=\vec{X}_0} \cdot \left(\tilde{a}_2\right) + \left.\frac{\partial f_{NL}(\vec{X})}{\partial \tilde{a}_2^*}\right|_{\vec{X}=\vec{X}_0} \cdot \left(\tilde{a}_2^*\right)\end{aligned} \qquad (4)$$

Assuming the PA is a nonlinear time-invariant system (NLTI), which implies that if the incident wave $\tilde{a}_1$ is phase shifted, the other waves will undergo the same phase shifting, which means that $\tilde{a}_1$ and $\tilde{a}_1^*$ depend on $|\tilde{a}_1|$ by introducing an arbitrary phase shifting $\phi(\tilde{a}_1)$. With these considerations, equation (4) can be written as:

$$\begin{aligned}\tilde{b}_i = S_i^0(|\tilde{a}_1|) + S_{i1}(|\tilde{a}_1|) \bullet \tilde{a}_1 + S_{i1}^{\Delta}(|\tilde{a}_1|) \bullet a_1^* \cdot e^{j2\phi(a_1)} + S_{i2}(|\tilde{a}_1|) \bullet \tilde{a}_2 \\ + S_{i2}^{\Delta}(|\tilde{a}_1|) \bullet a_2^* \cdot e^{j2\phi(a_1)}\end{aligned} \qquad (5)$$

Considering $\tilde{a}_1$ as the reference wave and that $\tilde{a}_2$ is negligible compared to $\tilde{a}_1$, equation (5) becomes:

$$\begin{pmatrix}\tilde{b}_1 \\ \tilde{b}_2\end{pmatrix} = \begin{pmatrix}S_{11}(|\tilde{a}_1|) & S_{12}(|\tilde{a}_1|) \\ S_{21}(|\tilde{a}_1|) & S_{22}(|\tilde{a}_1|)\end{pmatrix} \cdot \begin{pmatrix}\tilde{a}_1 \\ \tilde{a}_2\end{pmatrix} + \begin{pmatrix}0 & S_{12}^{\Delta}(|\tilde{a}_1|) \\ 0 & S_{22}^{\Delta}(|\tilde{a}_1|)\end{pmatrix} \cdot \begin{pmatrix}\tilde{a}_1^* \\ \tilde{a}_2^*\end{pmatrix} \qquad (6)$$

$S_{ij}(|\tilde{a}_1|)$ represent the nonlinear scattering functions that depend only on the incident wave magnitude. Equation (6) characterizes a bilateral nonlinear device, when $a_2 << a_1$. It can be seen as an AMAM - AMPM bilateral model, where the validity of the model remains limited to the operating frequency and inaccurate for moderate VSWR (VSWR ≥ 3). To solve the problem of model accuracy, we expanded the bilateral model to a Taylor development of second order. Considering once more $\tilde{a}_1$ as the reference wave and that $\tilde{a}_2$ is negligible compared to $\tilde{a}_1$, equation (6) is expanded and becomes:

$$\begin{aligned}b_1 &= S_{11} * \tilde{a}_1 + S_{12} * \tilde{a}_2 + S_{12}^{\Delta} * \tilde{a}_2^* + S_{12}^{\Delta'} * \tilde{a}_2^2 + S_{12}^{\Delta''} * \tilde{a}_2^{*2} + S_{12}^{\Delta''} * \tilde{a}_2 * \tilde{a}_2^* \\ b_2 &= S_{21} * \tilde{a}_1 + S_{22} * \tilde{a}_2 + S_{22}^{\Delta} * \tilde{a}_2^* + S_{22}^{\Delta'} * \tilde{a}_2^2 + S_{22}^{\Delta''} * \tilde{a}_2^{*2} + S_{22}^{\Delta''} * \tilde{a}_2 * \tilde{a}_2^*\end{aligned} \qquad (7)$$

B. Extraction procedure

The identification of nonlinear scattering functions defined in equation (6) consists of measuring the incident and the reflected power waves (Fig. 1), driven by a CW signal at the operating frequency of the PA in a load pull environment [5].

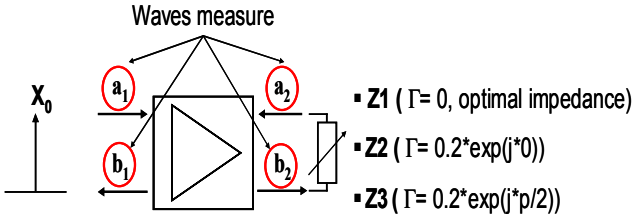

Fig. 1: Nonlinear Scattering Functions Extraction Setup.

In the case of the first order Taylor expansion, six parameters in equation (6) need to be extracted. To solve this system, it is necessary to make measurements for at least three different loading impedances having an orthogonal position on Smith chart and corresponding to a low mismatching (VSWR ≤ 1.6) in order to stabilize the system as well as possible.

Three load impedances are sufficient to solve the 3x3 linear system for different input powers, when PA is loaded with Z_{load}. The first measured impedance will be the reference; the other two measured impedances are located on a constant VSWR circle. The VSWR is between 1.3 and 1.6, and these values are chosen in order to have a large surface covered by those three impedances, but not large enough to make the system resolution unstable, so a compromise has to be done.

Otherwise, in the case of second order Taylor expansion, twelve parameters in equation (7) instead of six need to be extracted. The extraction is carried out by measuring the four power waves with six distinct impedances in order to solve the system. The selected impedances in this case are no longer orthogonally located. The first measured impedance will be the reference and the five other impedances are selected on a constant VSWR circle with an argument of 72 degrees compared to the previous chosen one.

III. Numerical Results

Those equations listed above enable us to establish a "black box" circuit model based on nonlinear scattering functions implemented into ADS (Agilent). The characterized device is

an 8-14 GHz 27dBm PA from NEX-TEC RF (NB00422), and no electrical model is provided by the manufacturer. The chosen operating frequency is 8.2GHz.

Both of the proposed models (first order and second order Taylor development) were identified on a scatter of measured impedances.

Extraction and validation of the first order model has been realized in ADS, through HB (Harmonic Balance) simulations at the operating frequency of the PA. The model has been implemented thanks to an FDD (Frequency-domain Defined Device) nonlinear block. The measured and identified S_{ij} functions are stored in a multi-dimensional "mdif" file format. The dimensions correspond to the real and imaginary part of the extracted S_{ij} and the fundamental frequency of the large-signal input tone. Equation (6) appears in a text file read by the model. A data-access component (DAC) links the tabulated data to the model and performs multidimensional interpolation during the simulation.

C. First order model validation

The fundamental AMAM and AMPM characteristics are compared in Fig. 2 and Fig. 3 for different chosen loads within the VSWR=2, VSWR=2.5 and VSWR=3 circle, showing the prediction ability of the PA model.

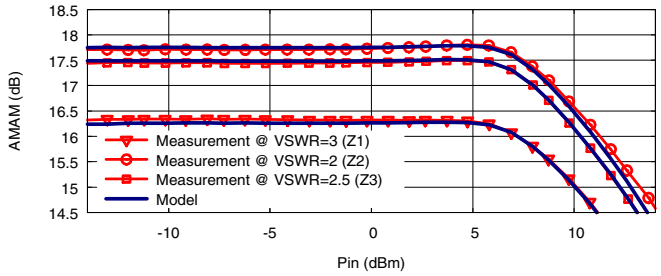

Fig. 2: Fundamental gain compression (AMAM) vs. input power for several impedances (Z1=16.5-j·7.5, Z2=37.4+j·21.1, Z3=39.9+j·40.1) on VSWR=2, 2.5 and 3 circle. Model (lines) compared to load pull measurement (symbols).

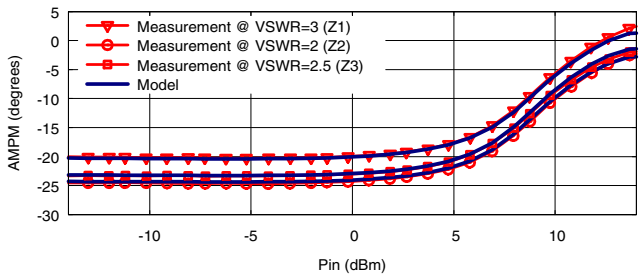

Fig. 3: Fundamental phase variation (AMPM) vs. input power for several impedances (Z1=16.5-j·7.5, Z2=37.4+j·21.1, Z3=39.9+j·40.1) on VSWR=2, 2.5 and 3 circle. Model (lines) compared to load pull measurement (symbols).

A good agreement is obtained between the PA model and the measurements. These results demonstrate the model capacities for predicting PA behavior up to VSWR=3. More experiments were performed in order to show the first order truncation, and Fig. 4 and Fig. 5 present the AMAM and AMPM responses on a VSWR=3.5 circle.

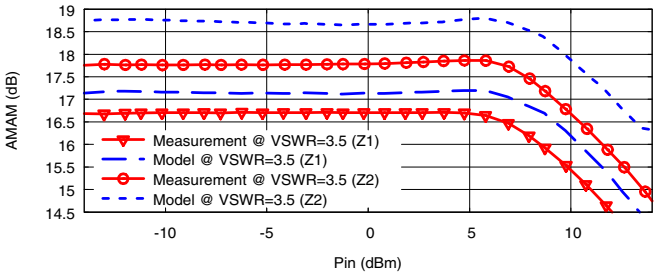

Fig. 4: Fundamental gain compression (AMAM) vs. input power for several impedances (Z1=23.8-j·31.5, Z2=48.4+j·56) on VSWR=3.5 circle. Model (lines) compared to load pull measurement (symbols).

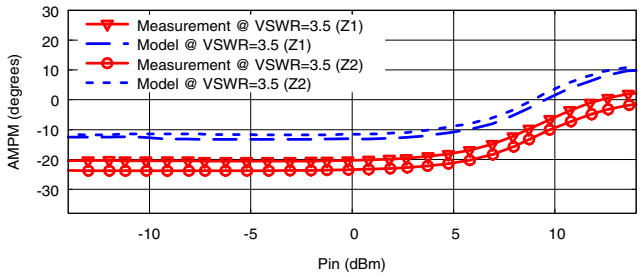

Fig. 5: Fundamental phase variation (AMPM) vs. input power for several impedances (Z1=23.8-j·31.5, Z2=48.4+j·56) on VSWR=3.5 circle. Model (lines) compared to load pull measurement (symbols).

Fig. 4 and Fig. 5, with important differences on AMAM and AMPM responses compared to previous figures with VSWR ≤3, show the limitations of the first order model. The second order model overcomes these limitations and improves model's accuracy, as it will be shown in the next section.

D. Second order model validation

The second order model is based on (7), and needs some modifications of the modeling process: to perform model extraction, six impedances (instead of three) located in the area of interest are now needed in order to cover the whole surface, but not large enough to make the system resolution unstable. Notice that the variation of $\tilde{a}_2$ is quadratic (not orthogonal) due to the impedances positions, which lead us to use a balanced algorithm (least squares optimization) in order to find the corresponding four waves.

Fig. 6 and Fig. 7 show the comparison between the behavioral model and the measurement in terms of gain (AMAM) and phase (AMPM) on VSWR=4 circle. It should be noted that the implementation process of the second order in ADS is not yet achieved due to the complexity of the model. The compared results were performed between the model algorithm and the measurement; no simulation was included. The global behavioral of PA model will indicate a remarkably good accuracy compared to the measurements.

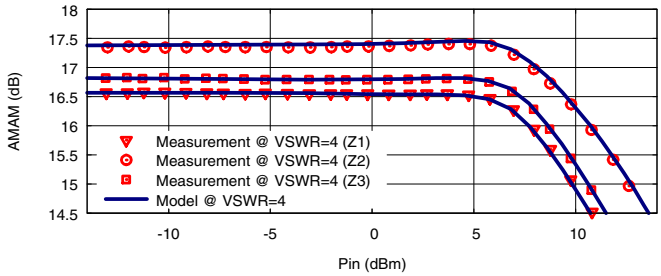

Fig. 6: Fundamental gain compression (AMAM) vs. input power for several impedances (Z1=15.7+j·22.3, Z2=21.5+j·35.8, Z3=40.2+j·63.9) on VSWR=4 circle. Model (lines) compared to load pull measurement (symbols).

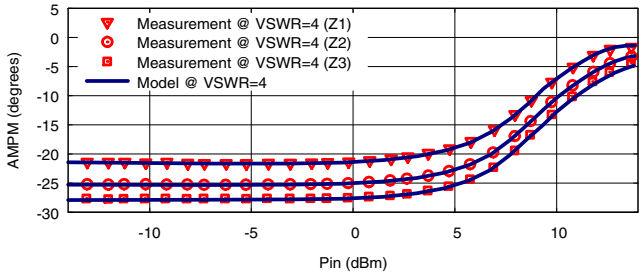

Fig. 7: Fundamental phase variation (AMPM) vs. input power for several impedances (Z1=15.7+j·22.3, Z2=21.5+j·35.8, Z3=40.2+j·63.9) on VSWR=4 circle. Model (lines) compared to load pull measurement (symbols).

The agreement is excellent, which demonstrate that the second order model is remarkably accurate, up to VSWR=4. Final experiments were performed using the impedances calculated with the electromagnetic code described earlier as load impedances. This study will enable us to observe the interaction between the antenna and the PA. Fig. 8 and Fig. 9 present the fundamental AMAM and AMPM response in the presence of some calculated impedances (antennas). Those calculated impedances correspond to high pointing angles (i.e. +35°, +40° and -35°) where their VSWR is between 2 and 3.

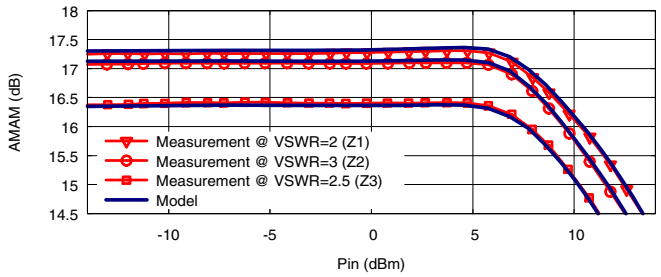

Fig. 8: Fundamental gain compression (AMAM) vs. input power for several calculated impedances (Z1=26.2j·0.004 (+40°), Z2=20.6+j·12.7 (-35°), Z3=21.6+j·18.8 (+35°)) using the electromagnetic analysis. Model (lines) compared to load pull measurement (symbols).

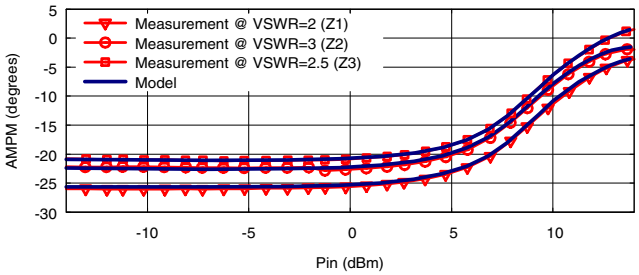

Fig. 9: Fundamental phase variation (AMPM) vs. input power for several calculated impedances (Z1=26.2j·0.004 (+40°), Z2=20.6+j·12.7 (-35°), Z3=21.6+j·18.8 (+35°)) using the electromagnetic analysis. Model (lines) compared to load pull measurement (symbols).

Fig. 8 and Fig. 9 show a perfect agreement. This approach demonstrates the prediction ability at system level and establishes a basic mixed simulation tool for a bilateral communication between amplifiers and antennas.

IV. Conclusion

We have presented two nonlinear behavioral models showing the prediction ability at system level for the PA's behavior subject to significant load mismatches (i.e. VSWR up to 4), as it may occur in agile antennas applications. We have demonstrated that the second order model is more efficient than the first order model (i.e. VSWR ≥ 3). The next step will be to implement the second order model into ADS and to extend the capacity of the behavioral model in order to take into account the memory effects (frequency dependence).

Acknowledgment

This work was realized within the framework of 'Lypsis project', labellized by the pole Elopsys (pole of competitiveness of high technologies in Limousin France - www.elopsys.fr), and supported by the French "Direction Générale des Entreprises".

References

[1] J. Drouet, M. Thevenot, R. Chantalat, C. Menudier, M. Koubeissi, T. Monédière, and B. Jecko, *"Global Synthesis Method for the Optimization of Multifeed EBG Antennas"*, International Journal of Antennas and Propagation, Vol. 2008, Article ID 790358.

[2] D.E. Root, J. Verspecht, D. Sharrit, J. Wood, A. Cognata, *"Broad-Band Poly-Harmonic Distorsion (PHD) Behavioral Models from Fast Automated Simulations and Large-Signal Vectorial Network Measurement"*, IEEE Transactions on Microwave Theory and Techniques, vol. 53, n°11, pp. 3656-3664, Nov. 2005.

[3] J.Verspecht, *"Scattering Functions for Nonlinear Behavioral Modeling in the frequency domain"*, Fundamentals of Nonlinear Behavioral Modeling, Foundations and Applications workshop, IEEE MTT-S, International Microwave Symposium, June 2003.

[4] G. Zakka El Nashef, F. Torres, A. El Sayed Ahmad, T. Monédière, M. Thévenot, S. Mons, E. N'Goya, R. Quéré, *"Development of an Electromagnetic Macro-model for Reconfigurable Array Application"*, 4th European Conference on Antennas and Propagation (EuCAP 2010), 12-16 April 2010, Barcelona, Spain.

[5] T. Reveyrand, A. Soury, F. Macraigne, G. Nanfack, D. Barataud, J.M. Nebus, E. N'Goya, *"A Time Domain Enveloppe Vectorial Network Analyser for Non-linear Measurement Based Modeling Accounting Impedance Mismatches"*, IMTC 2006 Instrumentation and Measurement, Technology Conference, 24-27 April Italy 2006.